The Coupled-Cavity Transmission Maser-Analysis

T. R. O'MEARA

Summary—This paper discusses an analysis of a maser amplifier structure (developed at Hughes Research Laboratories) consisting of a cascade of iris-coupled $\pi/2$ cavities intermixed with isolators. Starting from the basic media susceptibility, narrow-band equivalent networks and matrix representations are derived for maser and isolator cavities. A rational function approximation to the over-all gain function is thereby derived by matrix methods. From one viewpoint, the over-all amplifier may be regarded as a negative-resistance inverse-feedback amplifier. The key design parameter is shown to be the isolator round-trip attenuation. Excess isolation yields an overly rounded gain-frequency characteristic, while deficient isolation yields a characteristic with excess ripple or instability in the extreme cases. The feedback effects associated with intermediate "optimum" values of isolation reduce the effective gain per cavity below the normal gain of a single cavity, but in return one obtains a reduced gain sensitivity which may be reduced to a value comparable to or lower than that of the pure traveling-wave maser.

I. Introduction

THE MASER amplifier structure to be discussed in this paper is illustrated in Fig. 1. Details of construction are discussed in a companion paper [1]. It is a slow-wave microwave structure containing an activated or pumped-maser material with interspersed isolators, commonly known as a traveling-wave maser. From one viewpoint, the "slowing" structure slows the excitation wave sufficiently to permit a larger interaction with the maser material [2], [3], [4]. A less documented viewpoint is to regard maser gain as the reverse of incidental dissipation; as is well known, the first order effect of dissipation (or reverse dissipation) on the loss (or gain) function is proportional to group delay [5], and inversely proportional to circuit Q.

There exist a number of weak points in the usual slow-wave approach. The slow-wave structure power gain has been generally computed from the group velocity or slowing factor which, in turn, is generally computed on the assumption that there exists an image parameter match. Since the basic structures are not image terminated in an operational amplifier, the true group velocity near the band-pass edges and consequently the gain are subject to considerable doubt in conventional theory. In traveling-wave masers, the fundamental limitation on bandwidth has usually been set by the paramagnetic resonance line width rather than by the structure pass band. However, since the tunable bandwidth of a tunable maser *is* related to the structure bandwidth, it is important that this be accurately known.

In contrast to the slow-wave approach, passive microwave filters constructed of M structures, large in wavelengths ($\lambda/4$ or $\lambda/2$ dimensions are common), have been approximated by lumped-parameter networks with considerable success [6]. These equivalent lumped-parameter networks are much easier to analyze or synthesize than their distributed parameter counterparts.

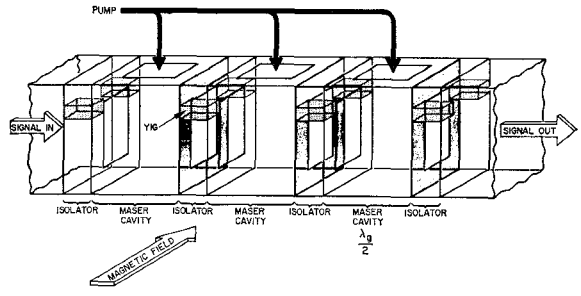

Fig. 1—The Hughes coupled-cavity maser amplifier structure.

This same general approach is also applicable to active filters including maser amplifiers, although so far as is known, it has not been previously attempted in the literature. With a filter approach, we may gain an understanding of many of the effects observed in the laboratory which are probably inexplicable by the usual traveling-wave concepts. For example, one may show how the maser activity and isolators influence bandwidth and band shape.

First we will develop a chain-matrix description of the three basic components which comprise the structure as follows: 1) the isolator, 2) the resonant active cavity, and 3) the coupling irises. These will be combined to obtain a matrix description of the over-all amplifier and its gain. Such a description yields the gain as a rational function of a frequency displacement variable, permitting more detailed analysis as well as an examination of a number of design problems.

The present analysis is basically concerned with an iterative structure, since we feel that the practical advantages of such structures outweigh their limitations. Furthermore, the active iterative filter, with proper control of the intercavity isolation, yields a much more satisfactory gain characteristic than the corresponding passive filter. The cryogenics present difficulty in tuning adjustments on an operating amplifier, providing one potent argument for structural simplicity.

II. Matrix Description of the Isolator

The isolators will be modeled by nonreciprocal transmission lines assumed to have the same characteristic impedance for waves in either direction and the same phase constant β but differing attentuation constants

Manuscript received October 2, 1963; revised February 24, 1964.
The author is with the Hughes Research Laboratories, Malibu, Calif.

α_1 and α_2. The electrical length will be assumed to be frequency independent.[1] Thus the isolator will be described by a chain matrix A_{is} such that

$$A_{is} = e^{\alpha_1 l_{is}} e^{-\alpha_{(+)} l_{is}} \cdot \begin{bmatrix} \cosh(\alpha_{(+)} + j\beta) l_{is} & Z_{is} \sinh(\alpha_{(+)} + j\beta) l_{is} \\ \frac{1}{Z_{is}} \sinh(\alpha_{(+)} + j\beta) l_{is} & \cosh(\alpha_{(+)} + j\beta) l_{is} \end{bmatrix} \quad (1)$$

where

$$\alpha_{(+)} = \frac{\alpha_1 + \alpha_2}{2}. \quad (2)$$

The isolator matrix A_{is} may be factored into a nonphase-shifting (or resistive) portion and a phase-shifting (or line-like) portion as indicated in Fig. 2. Thus

$$A_{is} = [\bar{A}][\tilde{A}_{is}] \quad (3)$$

where

$$A_{is} = e^{\alpha_1 l_{is}} \begin{bmatrix} \cosh(\theta/2) & Z_{is} \sinh(\theta/2) \\ \frac{1}{Z_{is}} \sinh(\theta/2) & \cosh(\theta/2) \end{bmatrix} e^{-\theta/2} \quad (4a)$$

$$\tilde{A}_{is} = \begin{bmatrix} \cos(\beta l)_{is} & jZ_{is} \sin(\beta l)_{is} \\ \frac{j}{Z_{is}} \sin(\beta l)_{is} & \cos(\beta l)_{is} \end{bmatrix} \quad (4b)$$

and

$$\theta = (\alpha_1 + \alpha_2) l_{is}. \quad (5)$$

The $\bar{A}_{is}$ matrix may be represented by various equivalent networks which must include gyrators or equivalent nonreciprocal elements.

Note that the isolator transmission line (of characteristic impedance Z_{is}) may be shifted "across" the $\bar{A}_{is}$ portion of the isolator because their matrices are commutative.

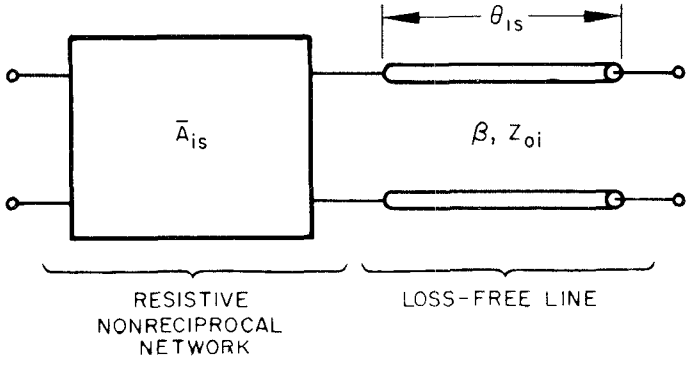

Fig. 2.

[1] The actual variation in electrical length with frequency introduces an additional bandwidth narrowing as in a passive filter [6] and may be included in much the same way, but only at the price of considerable complication in the analysis. This is because it becomes a selective element which, unlike the $\lambda_g/2$ cavity, is not activated.

III. A Network Description of the Maser Cavity Including the Coupling Irises

The passive isolator-deactivated structure strongly resembles the filters discussed by W. W. Mumford [6], although we consider iterative rather than maximally flat couplings. We would follow a modified Mumford analysis except for the following two reasons: 1) he derives an equivalent lumped-parameter resonator as a parallel tuned circuit rather than a series tuned circuit, and Kyhl [7], [8] has already illustrated a series type representation for a one-port $\lambda_g/2$ maser resonator which compares closely to our two-port circuit; and 2) we wish to make the transformer action of the irises explicit rather than implicit, as in Mumford's paper, because we feel this demonstrates more clearly their relation to the negative resistance gain.

A. The Maser Cavity

In the interest of brevity we will use a semiheuristic approach to the development of the narrow-band equivalent network for the masering cavity. A more rigorous (and lengthy) development based on transmission lines is presented O'Meara [1a]. First, note that masering action is usually a rather weak effect, the resulting imaginary component of the susceptibility being typically less than 1 per cent of the real part. Thus we look for an equivalent network based on a small perturbation of known equivalent network representations of passive $\lambda_g/2$ cavities. Such a cavity is conveniently represented in the low-pass case by a single series inductance plus an inverting transformer. This transformer, which plays no essential role in the operation of these amplifiers will be ignored in subsequent development. The impedance of the equivalent series element is [9], [10]

$$Z_c = s \frac{\pi K_g}{\omega_o Y_o} \quad (6)$$

where K_g is the guide wavelength factor

$$K_g = \left[1 - \frac{1}{\mu_r \epsilon_r} \left(\frac{\omega_c}{\omega_o}\right)^2\right]^{-1} \quad (7)$$

and Y_0 is the (passive) characteristic admittance of the guide. The frequency variable s represents the displacement from center frequency. Now, assuming that this equivalent inductance is the result of a magnetic energy storage throughout the masering volume, the active impedance should be directly proportional to the active permeability

$$\mu_r^* = \mu_r(1 + \chi) \quad (8)$$

where the susceptibility χ is assumed to be complex (as a result of masering action) and small (typically of the order of 10^{-2}). The susceptibility is assumed to be

$$\chi = \frac{j\chi_m''}{1 + j\tau\Delta\omega_m}. \quad (9)$$

where the parameter χ_m'' is the peak value of the absorptive-emissive component, τ is the reciprocal of the material half-line width, and

$$\Delta\omega_m = \omega - \omega_m \tag{10}$$

is the frequency departure from the material line resonance center frequency ω_m. Under these assumptions the masering impedance may be approximated as

$$Z_m \doteq \frac{\pi K_g}{\omega_o Y_o}\left[\frac{s^2 + s\left(s_{mo} + \frac{1}{\tau}\right) - \frac{\omega_o \chi_m''}{2\tau} + \frac{s_{mo}}{\tau}}{s + \frac{1}{\tau}}\right] \tag{11a}$$

where

$$s = j\Delta\omega_m = j(\omega - \omega_m) \tag{11b}$$

$$s_{mo} = j\omega_{mo} = j(\omega_m - \omega_o), \tag{11c}$$

and where ω_{mo} is the frequency displacement (if any) between the line resonance and the $\lambda_g/2$ resonant frequency, *i.e.*,

$$\omega_{mo} = \omega_m - \omega_o. \tag{11d}$$

If the cavity resonance frequency at ω_o and the line resonance at ω_m are synchronously tuned, the s_{mo} in (11a) vanishes, giving an effective series impedance

$$Z_m \doteq \frac{\pi K_g}{\omega_o Y_o}\left[s - \frac{\frac{\chi_m''\omega_o}{2\tau}}{s + \frac{1}{\tau}}\right]. \tag{12}$$

This impedance has one equivalent-network representation as illustrated in Fig. 3. When short circuited on one side, this network is a low-pass equivalent to the (one-port) Fig. 2 network of Kyhl [7], if Kyhl's series inductance is resonated.

On the other hand, if the maser line center frequency ω_m is tuned to the operating frequency ω as in a tunable maser[2] then s in (11a) vanishes giving

$$Z_m \doteq \frac{\pi K_g}{\omega_o Y_o}\left[s_{mo} - \frac{\chi_m''\omega_o}{2}\right]. \tag{13}$$

Now if we redefine s_{mo} in (13) as s, comparison to (12) demonstrates that we have in effect obtained infinite linewidth in our tunable maser. One may define an equivalent Q for this "tunable" maser by the definition

$$Q_{me} = \frac{\omega_o L_o}{2(R_m - R_o)} \doteq \frac{1}{\chi_m''}\left(1 - \frac{Q_o}{Q_m}\right)^{-1}. \tag{14}$$

The tunable situation, corresponding to (13), will be of dominant interest in this paper.

[2] This is most generally effected by changing the magnetic field.

B. The Coupling Irises

If the cavity were operated without coupling irises, the band-center frequency would be the $\lambda_g/2$ resonant frequency. However, the irises, which are needed to obtain reasonable gains, also introduce a detuning reactance X_{ir}, as may be seen from the equivalent transformer and transmission line representation[3] of Fig. 4. These iris reactances are easily eliminated by a frequency translation[4]

$$\bar{s} = s - j\frac{2X_{ir}}{L_o}, \tag{15a}$$

where for an equivalent iris line impedance of 1Ω

$$X_{ir} = \frac{b}{1 + b^2}. \tag{15b}$$

If δ_o is the percentage frequency shift associated with this translation, or in other terms the fractional separation between the $\lambda_g/2$ frequency and the operating frequency, then

$$\delta_o = \frac{-2X_{ir}}{\omega_o L_o} = \frac{-2b}{(1 + b^2)\pi K_g}. \tag{16}$$

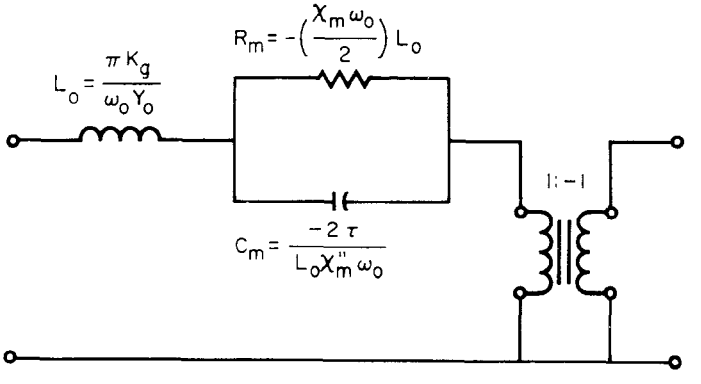

Fig. 3—An approximate lumped-parameter representation of a $\lambda_g/2$ maser cavity with the cavity synchronously tuned to the maser line.

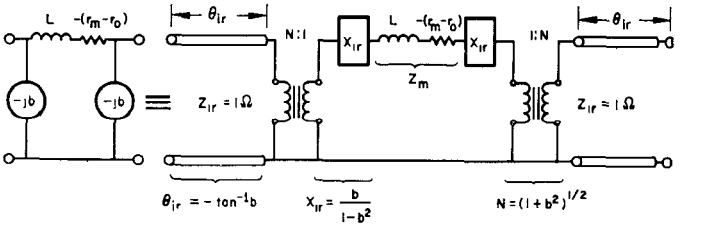

Fig. 4—Approximation equivalent network representation of the maser cavity and its coupling irises (with infinite linewidth).

[3] Note that all reactances and line lengths are assumed to be frequency independent in this representation. This network is a special case presented by G. G. Montegomery, *et al.*, Fig. (4.22a), p. 107, [9], with

$$Z_{11} = Z_{22} = Z_{12} = -jb^{-1}.$$

[4] This frequency translation is an expression of the iris detuning effect upon $\lambda_g/2$ cavity.

IV. The Effect of the Iris Transformers and the Effective Isolator Line Length

The ideal transformers of Fig. 4 may be removed by increasing all maser impedances by a factor of N, where

$$N^2 = 1 + b^2, \tag{17}$$

giving the equivalent network of Fig. 5 with an effective maser impedance, z_m, normalized to a one ohm cavity impedance, such that

$$z_m = N^2 Z_m = N^2(sL_o + R_o - R_m)\,Y_o. \tag{18}$$

The function of the iris-transformers can thus be regarded as that of increasing the effective negative resistance so that the effective power generated by the source current flowing through this negative resistance may be appreciable, compared with the source power. In this way, reasonable gains are obtained. In payment one accepts an enhanced inductance which reduces bandwidth. The maser-cavity-transformer portion of the microwave network may now be described by a transmission matrix

$$[A_m] = \begin{bmatrix} 1 & z_m \\ 0 & 1 \end{bmatrix}. \tag{19}$$

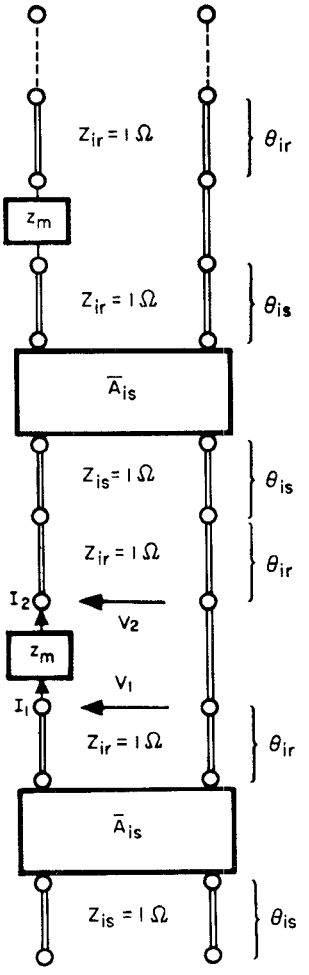

Fig. 5—A network representation for the combined amplifier.

The frequency independent lines at the beginning and the end of the amplifier of Fig. 5 introduce phase shifts only, but the internal lines are another matter. These lines may be shifted (as mentioned in section II) to either side of a reduced isolator and combined. Since we wish degenerative feedback at midband, the net phase shift in a signal passing round trip from one maser resistance through two irises and the isolator should be 180 degrees. In other terms, we require a total forward path (midband) phase shift of

$$\theta_{ie} = \theta_{is} + 2\theta_{ir} = \pm\,\pi/2 \text{ rad}. \tag{20}$$

Further, as will be shown, a frequency independent phase shift of $\pi/2$ is a sufficient condition for symmetry in the gain frequency function. From the equivalent network of Fig. 4, we see that the phase shift from two irises,

$$2\theta_{ir} = -\,2\tan^{-1} b, \tag{21}$$

is a function of b and hence of the required transformation ratio N. Thus (21) specifies the required isolator line length under normal circumstances.

Henceforth, the iris and isolator phase-shifting lines will be combined and considered as a portion of the isolator. Note that the forward attenuation $e^{\alpha_1 l_{is}}$ introduces only a loss constant, in the over-all transmission matrix, and will be ignored in subsequent development. Under these assumptions and with the isolator characteristic impedance normalized to one ohm, (3) may be written as

$$[A_{is}] = je^{-\theta/2}[\bar{\bar{A}}_{is}], \tag{22}$$

where

$$[\bar{\bar{A}}_{is}] = \begin{bmatrix} \sinh\theta/2 & \cosh\theta/2 \\ \cosh\theta/2 & \sinh\theta/2 \end{bmatrix}. \tag{23}$$

The j multiplier may be shifted to the end of the network or its matrix representation, resulting in an additional amplifier phase shift which, however, does not otherwise affect the amplifier gain characteristic. The remaining isolator matrix (23) still contains the both isolation properties and the impedance inverting properties normally associated with $\lambda_g/4$ lines.

V. The Gain-Frequency Function of the Over-All Amplifier and Some Degenerate Cases

Consider the over-all amplifier consisting of M-identical maser and isolator cavities coupled with identical irises, such as just discussed. One may avoid tedious expansions by utilizing the results of the existing theory of iterated networks [11], [12]. The simplest method commences with a unitary matrix as the basic transmission block. Thus, using (22) the over-all transmission

matrix for M cavities and M isolators[5] becomes

$$\begin{bmatrix} A_{11} & A_{12} \\ A_{21} & A_{22} \end{bmatrix} = e^{-M\theta/2}\{j[\overline{\overline{A}}_{is}][A_m]\}^M = (j)^M e^{-M\theta/2}\begin{bmatrix} \sinh\theta/2 & (\cosh\theta/2 + z_m \sinh\theta/2) \\ \cosh\theta/2 & (\sinh\theta/2 + z_m \cosh\theta/2) \end{bmatrix}^M \quad (24a)$$

where

$$z_m = p - d = N^2(sL_o + R_o - R_m)Y_o. \quad (24b)$$

The matrix elements in the expansion of (24a) are not of dominant interest. Rather, one desires the insertion gain expression.

$$g = \frac{2}{A_{11} + A_{12} + A_{21} + A_{22}} = \frac{2}{O_M}. \quad (25)$$

As shown by Armstrong [11], the denominator characteristic polynomial P_M is expressible as a sum of Chebyshev polynomials. Thus for source and load normalized to one ohm,

$$(j)^{-M} H^{-\frac{M}{2}} O_M = 2T_M(x) + (a_{12} + a_{21})U_{M-1}(x) = 2T_M(x) + \frac{2}{1+H}[j2H^{1/2} + x(1-H)]U_{M-1}(x), \quad (26a)$$

where a_{11}, a_{12}, a_{21} and a_{22} are the matrix elements of (24a),

$$H = e^{-\theta} \quad (26b)$$

and

$$x = \frac{1}{2}[a_{11} + a_{22}] = j\frac{H^{-1/2}}{2}\left[1 - H + (1+H)\frac{z_m}{2}\right]. \quad (26c)$$

By letting $p = j\Omega$ and expressing d in terms of an equivalent single cavity gain g_{os} a more useful expression for x is obtained

$$x = \frac{-H^{-1/2}}{2}\left[\frac{(1+H)\Omega}{2} - j\left(\frac{1+H}{g_{os}} - 2H\right)\right]. \quad (27)$$

Note that T_M and U_{M-1} in (26a) and (26b) are Chebyshev polynomials of the first and second kinds [13].

[5] It must be recognized that because of the extra isolator in the actual amplifier the forward gain or voltage transfer function will differ from that of (24a) by some phase shift factor. However, the magnitude of the forward gain function is not changed by these terminal isolators, except possibly for a small, constant reduction in gain resulting from forward isolator loss.

$$T_M(x) = \cos(M\cos^{-1}x) \quad (28a)$$

$$U_{M-1}(x) = \frac{\sin(M\cos^{-1}x)}{\sqrt{1-x^2}}. \quad (28b)$$

The second definition differs somewhat from that used by Armstrong [11].

Some properties of (26) are worth noting. Because T_M is of degree M while U_{M-1} is of degree $M-1$, one polynomial is even while the other is odd, and consequently $T_M(x)$ and $jU_{M-1}(x)$ are either both real or both imaginary (for real p or s). Thus the gain is a function of a polynomial in p with real coefficients and consequently the magnitude of the gain function is symmetrical (about $p/j = 0$), a consequence of our choice in effective isolator line length.

Several degenerate cases are of interest. If the isolators and the maser resistance are deactivated, then $H = 1$, $g_{os} = 1$ and (27) becomes

$$x = j\frac{z_m}{2} = j\frac{p}{2} = -\frac{\Omega}{2} \quad (29)$$

and the absolute value of the insertion gain reduces to

$$|g_o| = \left[1 + \left(\frac{\Omega}{2}\right)^2 U_{M-1}{}^2\left(\frac{\Omega}{2}\right)\right]^{-1/2}. \quad (30)$$

Allowing for the difference in notation in both frequency variable and the ordering of the Chebyshev polynomial (30) agrees with (186) of Lawson and Fano,[6] representing the $\lambda/4$-coupled cavity chain.

Let the isolation become very large, such that $H \to 0$. The gain function becomes

$$G = g^2 = \left(\frac{2}{p + 2 - d}\right)^{2M}. \quad (31)$$

Thus the over-all gain function becomes simply the product of the individual cavity gain functions.

Eq. (27) has been used to compute the characteristic polynomials, O_M,

$$O_M = \sum_{k_o}^{M} K_k(z_m)^k \quad (32)$$

corresponding to the inverse gain function, for M values 1 through 4. The results (powers of j are deleted) are as listed in Table I. Of particular interest is the fact that the constant term is $K_0 = 2$ (33) while the leading term is

$$K_m = \left(\frac{1+H}{2}\right)^{M-1}. \quad (34)$$

For $H = 1$ (no isolation) and $d = 0$, the filter reduces to a passive reciprocal filter with characteristic polynomials as listed by O'Meara [1a], [15].

[6] See page 681 of Ref. 14.

TABLE I
CHARACTERISTIC POLYNOMIALS OF THE ACTIVE FILTER

M	O_M
1	$= \frac{1}{2}[z_m + 2]$
2	$= \frac{1}{2}[(1 + H)z_m^2 + 4z_m + 4]$
3	$= \frac{1}{4}[(1 - H)^2 z_m^3 + 2(1 + H)(3 - H)z_m^2 + 12z_m + 8]$
4	$= \frac{1}{8}\{(1 + H)^3 z_m^4 + 2(1 + H)^2(4 - 2H)z_m^3 + 4(1 + H)(6 - 3H + H^2)z_m^2 + 32z_m + 16\}$
5	$= \frac{1}{16}\{(1 + H)^4 z_m^5 + 2(1 + H)^3(5 - 3H)z_m^4 + 4(1 + H)^2(10 - 8H + 3H^2)z_m^3 + 8(1 + H)(10 - 6H + 3H^2 - H^3)z_m^2 + 80z_m + 32\}$

VI. The "Optimum" Isolation Function for the General Amplifier

With more than two maser cavities, sufficient freedom does not exist under the assumptions (identical isolators and identical irises) to achieve any desired gain function, *e.g.*, equal ripple gain with prescribed ripple. Thus other techniques must be found for choosing the isolator round-trip attenuation to produce a desirable gain-frequency function. This is a central problem of this paper.

It is known from (31) that excess isolation results in a gain-function pole distribution with the poles nearly coincident [16], producing an excessively rounded gain-frequency function, with an excessively shrunken bandwidth. On the other hand, an extreme deficit of isolation will lead to instability. However, under-isolation has a more immediate effect in producing both a large gain peak at the band edges, and excessive ripple elsewhere in the pass band. An "optimum" intermediate value of isolation exists which compromises between these two conditions.

One method of choosing the isolator round-trip attenuation would be to establish first order flatness in the gain frequency characteristic. This technique proved prohibitively laborious, both in deriving equations and in solving them for $M > 4$. However, the $M = 2$ results are illustrated in Fig. 6. The $M = 2$, 3, and 4 cases are available to the interested reader in O'Meara's report [1a].

Some lower and upper bounds upon the isolation developed by O'Meara [1a] are illustrated in Fig. 6. Unfortunately, the limits are sufficiently widely spaced that the practical problem of finding an optimum H for a given g_{os} is not yet solved. However, it is possible to compute gain-frequency functions for specific cases and thereby estimate optimum isolation. As an example, consider the gain-frequency curves of a 10-cavity maser illustrated in Fig. 7. Observe that the optimum round-

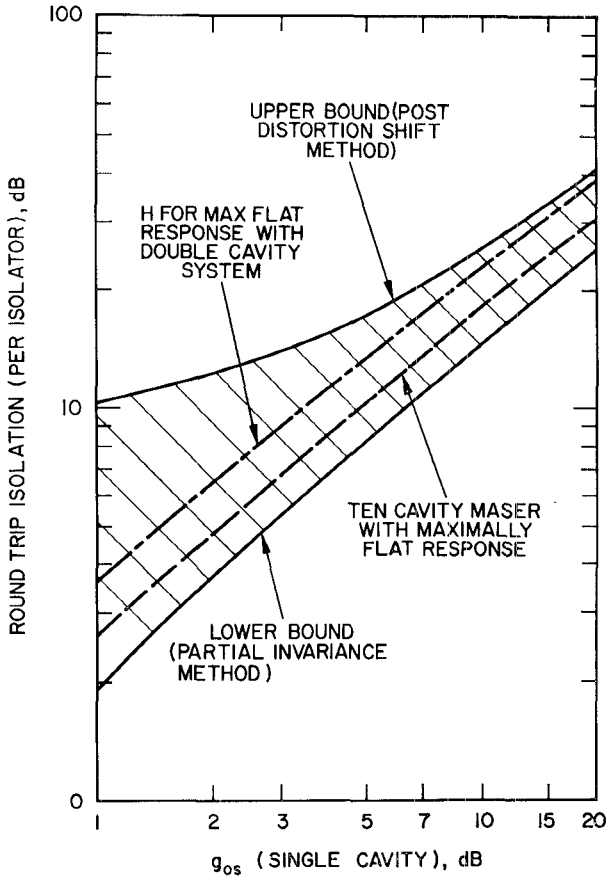

Fig. 6—Design ranges for optimum round-trip isolation.

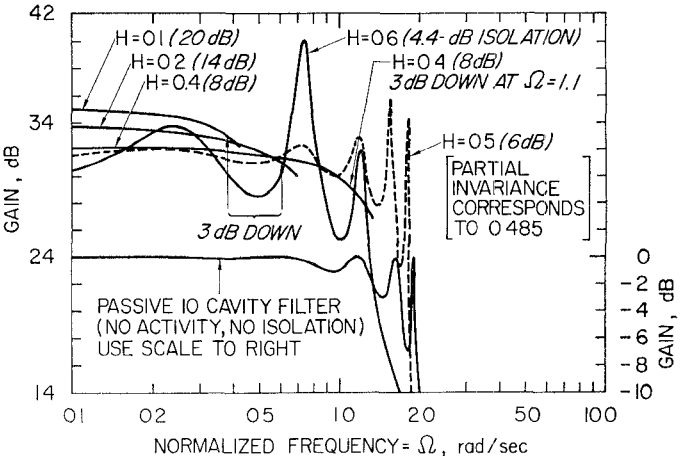

Fig. 7—Tunable-frequency-response for a ten cavity maser, $g_{os} = 1.53$.

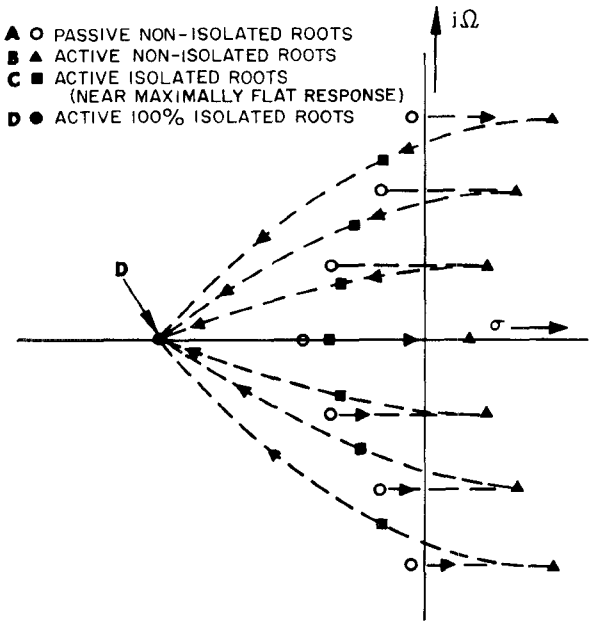

Fig. 8—A root-locus description of the isolater action (7-cavity amplifier).

trip isolation for this amplifier falls in the range[7]

$$0.4 < H < 0.43$$

and one pays a price in excess bandwidth shrinkage or excess gain ripple for H values which fall very far under or over these limits. From similar computations, it is estimated that near maximally flat isolation values fall on the design curves illustrated in Fig. 6.

Root locus concepts may serve to give a better understanding of the isolator function, as indicated in Fig. 8. The roots of $O_M(p)$, in the passive nonisolated case, will fall on a contour in the complex p-plane illustrated by position "A." If one first activates the amplifier, leaving the isolators inoperative, however, all roots are shifted equally[8] to the right in the p plane, with some or all of the roots shifting into the right half plane, as illustrated in the "B" position. Instability thereby results. The effect of large isolation is to make all the roots coalesce to a point "D" on the real or axis. Therefore, in the root locus migration, with increasing H, all roots must eventually cross back into the left half plane, restoring stability. The "optimum" H might thus yield the intermediate position illustrated as C of Fig. 8. This root-locus diagram also illustrates why the bandwidth of the final amplifier is less than that of the passive filter. The quantitative aspects of bandwidth shrinkage will be considered in a later section.

VII. Gain Loss

Unfortunately, the over-all effective band-center gain G_0 is only approximately given by the product of the individual cavity gains G_o'

$$G_o' = (g_{os})^{2M} = \left(\frac{2}{2-d}\right)^{2M} \tag{35}$$

since the inverse feedback action associated with nonvanishing H values reduces the gain somewhat below this value. This is a price one pays for the considerable gain bandwidth improvement and the slight sensitivity improvement associated with a proper choice in isolation. The over-all loss[9] in gain G_L may be expressed as

$$G_L = 20 \log_{10}\left[\frac{O_M}{O_M}\bigg|_{\substack{s=0\\H=0}}\right]$$

$$= 20 \log_{10}\left[1 - \left(\frac{g_{os}}{2}\right)^M F_M(H, d)\right] \tag{36}$$

where $F_M(H, d)$ is the difference in the polynomials O_M,

$$F_M(H, d) = 2^{M-1}\left[O_M\Big|_{s=0} - O_M\Big|_{\substack{s=0\\H=0}}\right]. \tag{37}$$

With normal designs, of moderate to large gain, the contributions of terms in (37) containing powers of H beyond the first are quite small and consequently a good approximation to (36) may be shown to be

$$G_L \doteq 20 \log_{10}[1 + (M-1)H(g_{os} - 1)^2] dB. \tag{38}$$

Table I compares some values of gain loss computed via (38) to the exact values. It is seen that (38) errs on the pessimistic side.

TABLE II
Some Computations of Gain Loss Resulting from Inverse Feedback

M	g_{os}	H	$g_o{}'$(db)	g_o(db)	G_L(db)	
					Exact	Via (38)
10	1.53	0.4	36.95	32.13	4.82	6.08
10	1.53	0.15	36.95	34.45	2.50	2.79
4	3.0	0.20	38.2	28.0	10.2	10.62
6	2.0	0.333	36.1	28.6	7.5	8.53

VIII. Tunable Bandwidth and Sensitivity

The basic reasons for using more than a single cavity in any negative resistance amplifier are twofold: 1) to improve gain bandwidth, and 2) to reduce the gain sensitivity to variations in activity (*e.g.*, pumping). Each of

[7] The value $H=0.43$ gives a single excess gain peak of approximately 0.12 db at $\Omega=0.190$, while $H=0.40$ is monotonic.

[8] Assuming all cavities are equally active. This is called a "predistortion" transformation in filter theory.

[9] This loss in gain is entirely from feedback action; the loss resulting from forward isolator attenuation must be computed and added separately.

these points will be discussed in more detail in the sections which follow.

A. Bandwidth Considerations

There are two aspects of tunable bandwidth to be discussed. The first involves the practical problem of finding the theoretical expected bandwidths of the activated, isolated amplifiers and of relating these bandwidths to other parameters, more easily measured, of the corresponding passive filter. The second aspect concerns the gain-bandwidths obtainable with this particular structure and compares these to some competitive amplifiers[10] and to theoretical limits.

Although most of the bandwidth measures given below will be given in terms of normalized bandwidth Ω_β, these are readily converted to true bandwidths via the equation

$$\overline{BW} = \frac{1}{4}\frac{\Omega_\beta \omega_o}{Q_{me}}\left(\frac{g_{os}}{g_{os}-1}\right) \tag{39}$$

where Q_{me} is the effective Q as already defined by (14).

It is convenient to have a means of finding the potential active bandwidth by passive (outside the dewar) measurements. The unloaded filter outer peaks shift but little with internal losses, providing a good measure of bandwidth. The outer peak is given by

$$\Omega_p = 2\cos\left(\frac{\pi}{M+1}\right). \tag{40}$$

In contrast, the outer peak of the loaded (passive lossfree) filter may be obtained from (30) as

$$\Omega_p' = 2\cos\left(\frac{\pi}{M}\right). \tag{41}$$

Although no general, exact formula for bandwidth has been found for the active-isolated amplifiers with intermediate values of isolation, there is a way of estimating bandwidth for responses which approach maximal flatness; that is, responses which are as flat as permitted by the constraints. Note from (26) that the gain is of the form

$$g = 2[K_M p^M + \cdots \overline{K}_o]^{-1} \tag{42}$$

where K_M is as given by (34) while K_o is the summation of K_o, as defined in (33), plus the contributions from d in the other terms of (32). Consequently, the midband gain is

$$g_o = 2(\overline{K}_o)^{-1}. \tag{43}$$

[10] It is the gain-tunable bandwidth of the maser which compares most nearly with the (instantaneous) gain-bandwidth of the tunnel diode and the parametric amplifier.

If the maximally-flat response condition yields a distribution of poles approximating a semicircle in the left hand p plane (*i.e.*, a pseudo-Butterworth distribution) then the mean radius of this circle, which is obtained from the product of the complex roots, is a good measure of the 3 db half bandwidth.[11] Thus, the normalized full "Ω" bandwidth is approximately

$$\Omega_\beta \doteq 2\left(\frac{\overline{K}_o}{K_M}\right)^{1/M} = 4g_o^{-1/M}(1+H)^{(1-M)/H}. \tag{44}$$

This full bandwidth may be normalized relative to the 3 db full bandwidth of a single passive cavity, giving

$$\Omega_{\beta r} \doteq g_o^{-1/M}(1+H)^{(1-M)/M}. \tag{45}$$

For $M=2$ the bandwidth expression (45) is exact. As another example, the isolation value of $H=0.4$ which corresponds very closely to a maximally-flat response with 32 db gain in a 10-cavity maser, yields a normalized ($\Omega_{\beta r}$) bandwidth of 0.505 while (45) predicts a bandwidth of 0.502. By increasing H to 0.43 one may widen the relative bandwidth to approximately 0.615 at the price of a 0.12 db gain ripple over the bandwidth. Although the bandwidth shrinks less rapidly than with a 100 per cent isolated system, it still remains smaller than that of the passive filter.

Substituting (39) in (45) gives the (denormalized) relative bandwidth B_r as

$$B_r = \frac{1}{Q_{me}}\left(\frac{g_{os}}{g_{oe}}\right)\frac{(1+H)^{(1-M)/M}}{(g_{os}-1)}. \tag{46}$$

The resulting increase in B_r with increasing M is illustrated[12] in Fig. 9. The increase with M is very rapid at first, becoming nearly linear at higher values of M. The limiting behavior is explored in the Appendix. It is therein shown that for large M

$$(B_r Q_{me}) \approx \frac{M}{\ln G_o}. \tag{47}$$

This value is illustrated in Fig. 11 and therein compared to more exact curves based on specific computer results.

It is interesting to compare (47) with one kind of theoretical limit, which is structure independent. As mentioned in the introduction, maser negative resistance gain action may be regarded as a type of inverse incidental dissipation. It has been long known that small values of incidental dissipation (either positive or

[11] As the actual critical frequency distributions tend to be somewhat elliptical (which the major axis in the Ω direction) this assumption generally gives a pessimistic estimate of bandwidth for $M>10$. However, computer checks indicate that (44) is a good compromise for most design values.

[12] The curves are based on specific values of M, g_o, and H associated with specific computer examples.

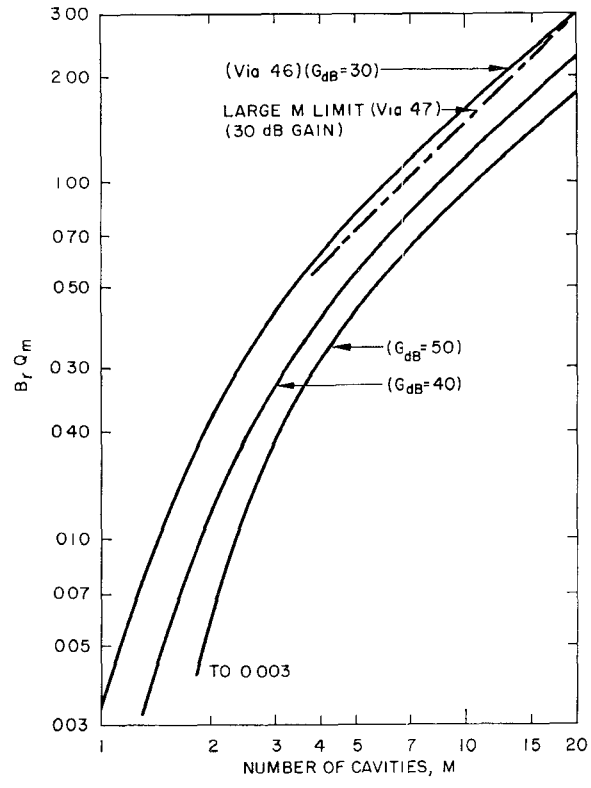

Fig. 9—Some approximations to tunable percentage bandwidth as a function of number of cavities (with constant over-all gain as a parameter).

negative) may be well approximated in terms of the group delay function T_g, and the cavity Q of a band-pass filter as [5], [19]

$$G_{dB} \doteq \frac{8.69\omega_o T_g(\omega_o)}{2Q} . \tag{48}$$

Now it is also known that the maximum uniform group delay which can be obtained from M resonators may be related to the bandwidth (in cycles) B_g, over which the delay is uniform, by the formula [20]

$$T_g B_g = \frac{\eta M}{2} < \frac{M}{2} \tag{49}$$

while η is a delay area efficiency. Combining (48) and (49) one may derive

$$B_r Q = \eta \frac{\pi}{2} \frac{M}{\ln G_o} \tag{50}$$

which compares closely to, but is somewhat larger than (47), for large η.

An equation may be derived for the direct-coupled Butterworth response maser [21] which, in the limit of large M and large $B_r Q_m$, reduces to the same form as (47). Thus, as shown by O'Meara [1a], one obtains

$$\lim_{M\to\infty} B_r Q_{me} = \frac{4}{\pi}\left(\frac{M}{\ln G_o}\right) \tag{51}$$

giving a gain-bandwidth factor 27 per cent greater than that of the isolator-coupled maser. Actually, for a typical design (an $M=10$ and $B_r Q=1.6$) (51) gives an optimistic result while (47) is pessimistic; the gains are nearly identical (33.2 db vs 32.13 db).

Gain-bandwidth may also be increased by compensation with passive network elements [22], [23] (*i.e.*, cavities). However, as one usually does not double the bandwidth (a 30 per cent increase is more typical) by doubling the total number of elements (one passive for each active element) and as it costs little more to insert an active as opposed to a passive cavity in a dewar, it appears that there is very little point to these compensation schemes with masers.[13]

B. Sensitivity

A fundamental problem with all negative-resistance amplifiers is that small changes in negative resistance or loading produce relatively large changes in gain. The maser amplifier provides no exception, although it is usual to operate in a saturated condition such that changes in pump power have relatively little influence on negative resistance [16].

While the computation of the exact gain sensitivity is, in general, tedious, some special cases are relatively simple. The easiest is for infinite ($H=0$) isolation. With infinite isolation, the over-all band-center gain G_o is given by (35). Thus the gain sensitivity $S^{G}_{r_m}$ at band benter with respect to changes in R_m (or x_m'') is [1a][14]

$$S_{r_m}^{G_o}(\Omega = 0)\frac{dG_o/G_o}{d(r_m)/r_m} = g_o M(d + R_o)$$

$$= 2M(G_o^{1/2M} - 1)\left(\frac{R_m}{R_m - R_o}\right). \tag{52}$$

This result agrees with Stitch's (20C) [18], with $M=1$, as it should. On the other hand, as M becomes large it is readily shown that

$$\lim_{M\to\infty} 2M(G_o^{1/2M} - 1) = \ln G_o \tag{53}$$

and, therefore

$$\lim_{M\to\infty} S_{r_m}^{G} = \left(\frac{r_m}{r_m - r_o}\right)\ln G_o \tag{54}$$

[13] It should be emphasized that we refer only to the problem of increasing tunable bandwidth. Compensating for instantaneous bandwidth is another matter.

[14] The corresponding sensitivity for a coupled series of reflection type cavities is given by Kyhl and Strandberg [17] (in the notation of this paper as $(dG_o/G_o)(dr_m/rm) = M(G^{1/2M} - G^{-1/2M})$. The M factor in Strandberg's (15) was omitted and he presumes $r_o=0$. The reflection type cavity series has the advantage for low values of M, but this advantage rapidly vanishes as M becomes modestly large.

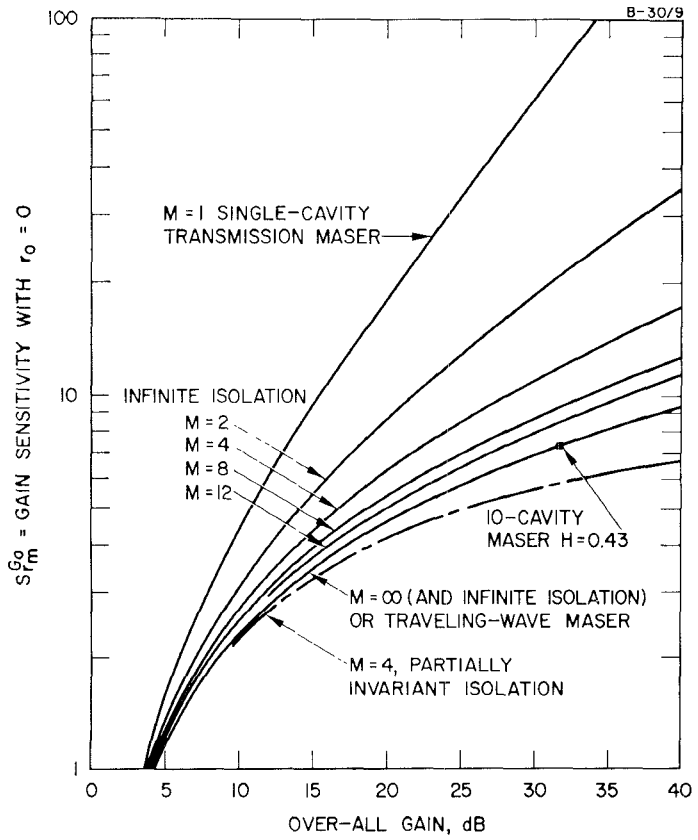

Fig. 10—Gain sensitivity of coupled cavity masers to variations in activity.

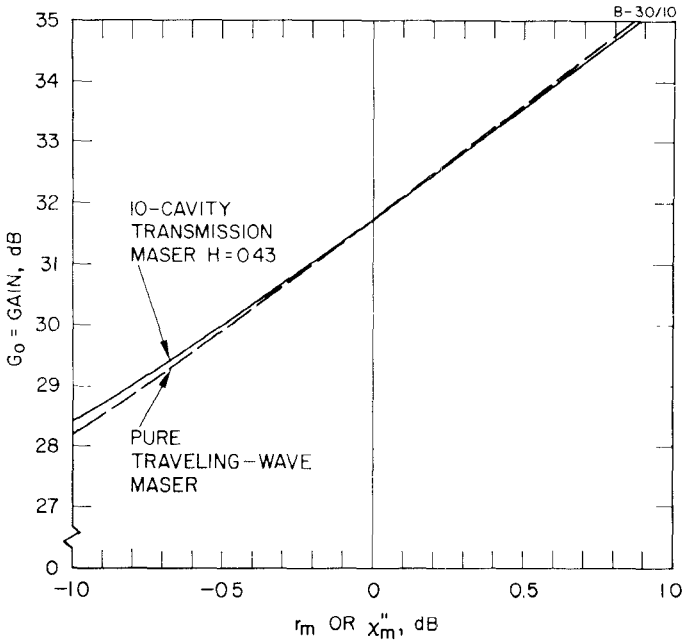

Fig. 11—Decibel gain changes of a 10-cavity maser as a function of db changes in activity.

which is the same result as for the traveling wave maser, as given by De Grass, *et al.* [2], if residual losses are included in the traveling-wave formula. Ignoring the factor $[R_m/R_m - R_o)]$, the $H=0$ sensitivities for $M=1$, 2, 4, 8, 12 and ∞ have been computed from (53) and (54) and plotted in Fig. 10. It is seen that M does not have to be very large before the traveling-wave sensitivity is approached rather closely.

None of these results has obtained any advantage from the potential inverse feedback action associated with finite values of isolator ratio. Some special cases are discussed by O'Meara [1a] and one of these is illustrated in Fig. 10. One sees that improvement is possible and one may decrease the sensitivity slightly below that of the traveling wave maser. However, the case illustrated corresponds to more feedback than one can afford to use from a gain-frequency control viewpoint.

The sensitivity with a value of isolation corresponding to a near optimum H in a 10-cavity maser has been computed for one particular gain value (31.7 db) and is plotted as a single point in Fig. 10. It falls almost on top of the curve for the traveling-wave maser.

One may question if the sensitivity is a good measure of the actual gain changes and if so over what ranges. Fig. 11 compares the actual gain changes occurring with a 10-cavity maser and a pure traveling-wave maser for variations in r_m measured in db. It is seen that the two curves are nearly identical with the 10-cavity maser having an almost insignificant advantage. As both curves are nearly linear over a range of ± 1 db variation in R_m (or χ_m''), the sensitivity is indeed a good measure. Similar computations near the band-edge frequencies of the 10-cavity maser yield lesser variation in gain.

IX. Conclusions

The maser amplifier which has been analyzed proves to be fairly complex in spite of numerous approximations and the fact that many degrees of freedom have been eliminated by the choice of an iterative structure. Consequently, exact theoretical formulae are not available for all parameters of interest. However, certain interim conclusions may be drawn. Probably the four most significant conclusions are the following:

1) Unlike the nonisolated iterative passive filter, the band-pass ripple may be held to quite low values by the proper choice in round-trip isolation.
2) The product of gain in db and relative bandwidth is linearly proportional to the number of cavities (in first order theory) if the number of cavities is reasonably large, given optimal isolation values.
3) The gain-tunable-bandwidth product obtainable with this structure is comparable to that obtained with competitive structures (using equally active cavities or reactive elements).

4) It may often be good practice to employ a larger number of cavities than dictated by gain-bandwidth requirements in order to improve stability, that is, to reduce the sensitivity to cavity loadings or activity (*e.g.*, pumping).

Although we have not succeeded in developing exact formal equations for either round-trip isolation or bandwidth, by combining computer results and various approximations we have been able to prepare design curves which should permit a choice in these parameters sufficient for normal engineering applications.

Appendix

Limiting Gain-Bandwidth as the Number of Resonators Becomes Large

From (46), it is noted that

$$B_r Q_{me} = \left(\frac{g_{os}}{g_{oe}}\right)\left(\frac{1+H}{g_{os}-1}\right)^{(1-M)/M}. \tag{55}$$

Also note that the difference between g_{oe} and g_{os} is a second order effect in the parameter $(\ln G_o/2M)$. Specifically, it is readily derived from (38) that

$$1-\frac{g_{oe}}{g_{os}} \approx H\left(\frac{\ln G_o}{2M}\right)^2 \approx \left(\frac{\ln G_o}{2M}\right)^2. \tag{56}$$

Second, note from Fig. 6 that an optimum H is related to g_{os}, roughly as

$$\ln H \approx -K \ln g_{os} \tag{57}$$

where K is a constant whose exact value is uncertain, but lies roughly in the range

$$2 < K < 2.5. \tag{58}$$

Using a series expansion for H values near unity and ignoring the second order distinction between g_{oe} and g_{os} gives

$$1+H \approx 2-K\ln g_{oe} = 2\left(1-\frac{K\ln G_o}{4M}\right). \tag{59}$$

Since the $g_{os}-1$ factor in (55) is small to begin with, second-order corrections of the form (56) become important. Thus

$$\frac{g_{os}}{g_{oe}}(g_{os}-1)^{-1} \approx \left[1-\frac{g_{oe}}{g_{os}}+\frac{\ln G_o}{2M}\right]^{-1} \approx \frac{2M}{\ln G_o}\left[1+\frac{\ln G_o}{2M}\right]^{-1}. \tag{60}$$

Substituting (59) and (60) in (55) gives a large M approximation

$$B_r Q_{me} \approx \frac{M}{\ln G_o}\left[1+\left(1-\frac{K}{2}\right)\frac{\ln G_o}{2M}\right]^{-1} \approx \frac{M}{\ln G_o}. \tag{61}$$

List of Symbols

$A_{11}, A_{12}, A_{21}, A_{22}$ — Matrix element of the over-all amplifier matrix.

A_{is} — Transmission matrix description of an isolator.

$\bar{\bar{A}}_{is}$ — A reduced isolator matrix which includes the inversion and isolation functions of an effective $\lambda/4$ isolator but excludes phase shift effects.

$\bar{A}_{is}$ — The resistive part of an isolator matrix.

A_m — Transmission matrix describing a maser cavity.

$b = B/Z_o$ — Normalized iris susceptance.

$B_r = \dfrac{\omega_{3db} - \omega_{db3}}{\omega_o(1+\delta)}$ — Relative bandwidth of an M-cavity maser.

$d = N^2(r_m - r_o)Y_o$ — A transformed effective maser cavity resistance; also a predistortion shift in the complex frequency plane (assuming a normalized cavity inductance of 1 Henry).

$g_o = \sqrt{G_o}$ — Band-center transducer voltage gain of an M-cavity maser.

g_{os} — Band-center transducer voltage gain of a single-cavity maser.

G_L — Gain loss (in db) as a result of inverse feedback action.

$g_{oe} = (g_o)^{1/M}$ — Band-center effective transducer voltage gain of a single-cavity in an M-cavity maser.

G_{db} — Over-all power gain in db.

$H = \exp(\alpha_1 + \alpha_2)l_{is}$ — Round-trip attenuation of a single isolator as a voltage ratio.

$K_g = (\lambda_g/\lambda)^2 = \left[1 - \dfrac{1}{\mu_r\epsilon_r}\left(\dfrac{\omega_c}{\omega_o}\right)^2\right]^{-1}$ — Guide wavelength factor.

$L_o = \dfrac{\pi K_g}{\omega_o Y_o}$ — Equivalent low-pass inductance of a $\lambda/2$ cavity.

M	Number of maser cavities.
$N = 1 + b^2$	Turns ratio of the effective transformer in a transformer and line representation of an iris.
$O_M = \sum K_k(z_m)^k$	A polynomial in z_m, whose reciprocal gives the transducer gain.
$p = \sigma + j\Omega$	Normalized low-pass complex frequency variable.
$Q_m = \dfrac{1}{\chi_m''} = \dfrac{\omega_o L}{2R_m}$	Maser medium Q.
$Q_{me} = \dfrac{\omega_o L}{2(R_m - R_o)} = \left[\dfrac{1}{\chi_m''}\left(1 - \dfrac{R_o}{R_m}\right)\right]^{-1}$	Effective Q of a resonant network representing a waveguide filled with a medium having a susceptibility x_m.
R_o	A residual (passive) loss resistance in a $\lambda/2$ maser cavity resulting from wall or dielectric losses.
R_m	A resistance introduced by the maser action within a material filling a waveguide.
s	A low-pass or displacement complex frequency variable.
$s_{mo} = j(\omega_m - \omega_o)$	Frequency displacement between the line resonance center frequency and the (iris-short-circuit) cavity resonant frequency.
$S_l^k = \dfrac{d[\ln k]}{d[\ln l]}$	Sensitivity of k to the parameter l.
$T_M(x) = \cos(M \cos^{-1} x)$	Chebyshev polynomial of the first kind.
$U_{M-1}(x) = \dfrac{\sin(M \cos^{-1} x)}{\sqrt{1 - x^2}}$	Chebyshev polynomial of the second kind.
$x = j\dfrac{H^{-1/2}}{2}\left[1 - H\ (1 + H)\dfrac{z_m}{2}\right]$	Complex argument of a Chebyshev polynomial.
X_{ir}	Equivalent series reactance resulting from an iris susceptance.
$Y_o = (Z_o)^{-1}$	Characteristic admittance of a passive waveguide or line.
$Z_m = sL_o + R_o - R_m$	Effective series impedance representing a $\lambda/2$ maser cavity.
$z_m = N^2 Z_m Y_o = p - d$	Effective transformed low-pass impedance of a $\lambda/2$ maser cavity, normalized to the waveguide characteristic impedance of.
α_1	Forward path attenuation constant in an isolator-waveguide section.
α_2	Backward path attenuation constant in an isolator-waveguide section.
$\alpha_{(+)} = \dfrac{\alpha_1 + \alpha_2}{2}$	Average attenuation constant.
$\delta = \delta\omega/\omega_o$	Relative frequency shift resulting from iris detuning.
$\Delta\omega_o = \omega - \omega_o$	A frequency departure from the $\lambda/2$ resonant frequency.
$\Delta\omega_m = \omega - \omega_m$	A frequency departure from the material line center frequency.
$\omega_{mo} = \omega_m - \omega_o$	Frequency displacement between the line resonance and the $\lambda_g/2$ resonant frequency.
$\theta = \ln H = (\alpha_1 + \alpha_2)l_{is}$	Round-trip attenuation of a single isolator in nepers.
θ_{is}	Electrical length of the isolator, in radians.
θ_{ir}	Electrical length of the effective line in a transformer and line representation of a single iris.
λ_g	Guide wavelength.
μ_r	Relative permeability of a passive medium.
$\mu_r^* = \mu_r(1 + \chi)$	Complex permeability of an active maser medium.
τ	Maser material reciprocal half-line width.
χ	Complex susceptibility of a maser medium.
χ_m''	Peak value of imaginary part of χ.

ω	Band-pass frequency variable.
ω_c	Cutoff frequency in a waveguide.
ω_m	Maser medium line center frequency.
ω_o	Passive iris-short-circuit $\lambda/2$ resonance frequency of a line or cavity.
Ω	A normalized low-pass frequency variable.
Ω_p	Outer-peak (normalized) frequency of a loss-free unloaded passive filter.
Ω'_p	Outer-peak (normalized) frequency of a loss-free loaded passive filter.

Acknowledgment

The author wishes to thank K. Higa of the Hughes Computing Department, Malibu, Calif., for programming and running the computations leading to the preparation of Fig. 7.

References

[1a] T. R. O'Meara, "An Analysis of the Isolator-Coupled-Cavity Transmission Maser, Parts I and II," Hughes Research Labs., Malibu, Calif., Research Rept. No. 259; April, 1963.
[1b] F. E. Goodwin, J. E. Kiefer and G. E. Moss, "The Coupled-Cavity Transmission Maser—Engineering Design," Hughes Research Labs., Maliblu, Calif., Research Rept. No. 252; August, 1962.
[2] R. W. DeGrasse, E. O. Schulz-DuBois, and H. E. O. Scovil, "The three-level solid state traveling-wave maser," *Bell Sys. Tech. J.*, vol. 39, pp. 1–47; March, 1959.
[3] "Solid-State Maser Research Report No. 2," Bell Telephone Labs. Contract No. DA-36-039 SC-85357, 2nd Quarterly Rept.; December 20, 1960.
[4] A. E. Siegman, "Microwave Solid State Masers," McGraw-Hill Book Co., Inc., New York, N. Y.; 1964.
[5] H. W. Bode, "Network Analysis and Feedback Amplifier Design," D. Van Nostrand Co., Inc., New York, N. Y., pp. 216–222; 1945.
[6] W. W. Mumford, "Maximally flat filters in waveguide," *Bell Sys. Tech. J.*, vol. 27, pp. 648–714; October, 1948.
[7] R. L. Kyhl, R. A. McFarlane, and M. W. D. Strandberg, "Negative L and C in solid-state masers, "Proc. IRE, vol. 50, pp. 1608–1623; July, 1962.
[8] R. L. Kyhl, "Negative L and C in solid-state masers," Proc. IRE, (*Correspondence*), vol. 48, p. 1157; June, 1960.
[9] C. G. Montgomery, R. H. Dicke and E. M. Purcell, "Principles of Microwave Cicruits," M.I.T. Rad. Lab. Ser., McGraw-Hill Book Co., Inc., New York, N. Y.; 1948.
[10] S. B. Cohn, "Direct-coupled resonator filters," Proc. IRE, vol. 45, pp. 187–196; February, 1957.
[11] H. L. Armstrong, "Note on the use of Tchebyscheff functions in dealing with iterated networks," IRE Trans. on Circuit Theory, vol. CT-2, pp. 169–170; June, 1955.
[12] L. Storch, "On the chain matrix of cascaded networks," IRE Trans. on Circuit Theory (*Correspondence*), vol. CT-3, pp. 297–298; December, 1956.
[13] "Tables of Chebyshev Polynomials $S_n(x)$ and $C_n(x)$", U. S. Dept. of Commerce, National Bureau of Standards, Applied Mathematics Series, U. S. Government Printing Office, Washington, D. C., 1952.
[14] G. L. Ragan, "Microwave Transmission Circuits," vol. 9, M.I.T. Rad. Lab. Ser., McGraw-Hill Book Co., Inc., New York, N. Y.; 1948.
[15] T. R. O'Meara, "Generating arrays for ladder network transfer functions," IEEE Trans. on Circuit Theory (*Correspondence*), vol. CT-10, p. 285; June, 1963.
[16] G. E. Valley and H. Wallman, "Vacuum Tube Amplifiers," vol. 18, M.I.T. Rad. Lab. Ser., McGraw-Hill Book Co., Inc., New York, N. Y.; 1948.
[17] M. W. P. Strandberg, "Unidirectional paramagnetic amplifier design," Proc. IRE, vol. 48, pp. 1307–1320; July, 1960.
[18] M. L. Stitch, "Maser amplifier characteristics for transmission and reflection cavities," *J. Appl. Phys.*, vol. 29, pp. 782–789; May, 1958.
[19] E. A. Guillemin, "Communication Networks," John Wiley and Sons, New York, N. Y. vol. II, pp. 445–448; July, 1947.
[20] E. S. Kuh, "Synthesis of lumped parameter precision delay lines," Proc. IRE Convention Record, vol. 45, pp. 160–174; December, 1957.
[21] L. Weinberg, "Synthesis using tunnel diodes and masers," IRE Trans. on Circuit Theory, vol. CT-8, pp. 66–75; March, 1961.
[22] H. J. Carlin, *et al.*, "Comments on design theory of optimum negative-resistance amplifiers," Proc. IRE, vol. 49, pp. 1687–1688; November, 1961.
[23] D. C. Youla and L. I. Smilen, "Optimum negative-resistance amplifiers," Proc. Symp. on Active Networks and Feedback Systems, Polytechnic Press, Polytechnic Inst. of Brooklyn, N. Y.; April 19–21, 1960.